FOI

Comparison of Two Mobility Models for Tactical Ad Hoc Networks

ULF STERNER

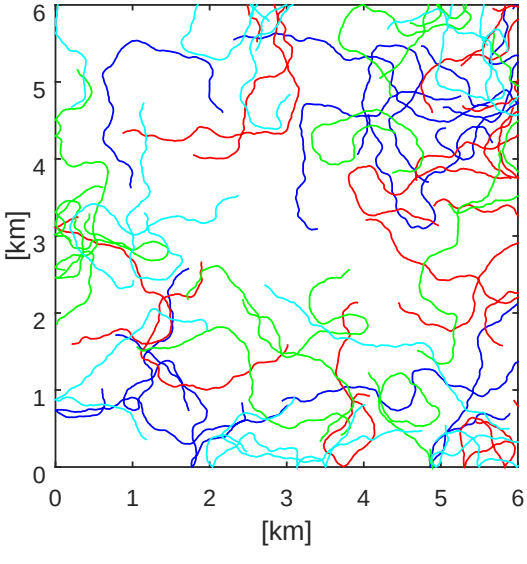

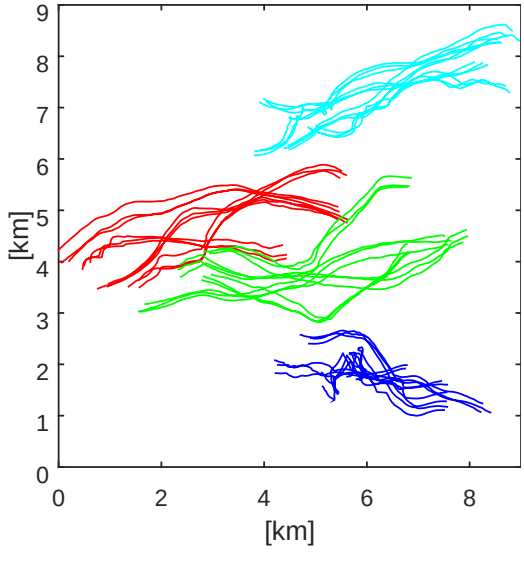

FOI-R--4220--SE
ISSN 1650-1942 January 2016

Ulf Sterner

Comparison of Two Mobility Models for Tactical Ad Hoc Networks

Titel	Jämförelse av två mobilitesmodeller för taktiska ad hoc-nät
Title	Comparison of Two Mobility Models for Tactical Ad Hoc Networks
Rapportnr / Report No.	FOI-R--4220--SE
Månad / Month	Januari / January
Utgivningsår / Year	2016
Antal sidor / Pages	33
ISSN	1650-1942
Kund / Customer	FMV
Forskningsområde	4. Informationssäkerhet och kommunikation
FoT område	Ledning och MSI
Projektnr / Project No.	E324531
Godkänd av / Approved by	Christian Jönsson
Ansvarig avdelning	Ledningssystem

Abstract

When modelling tactical radio networks it is important to capture the effects of the nodes' mobility. Here we compare a tactical scenario with two mobility models, a random walk model and a group mobility model. Compared to the random walk model, the group model offers more adjustment options but has a more complex model structure.

Evaluation of a basic waveform shows that the group mobility model is less challenging than the random walk model in terms of available capacity, but more challenging in terms of delivery ratio. The group model also requires more or longer simulations compared to the random walk model to obtain the same variance of the evaluated metrics. Furthermore, the evaluation shows that the radio channel and the used terrain area usually have much more effect on the simulation result than the movement patterns of the nodes. Thus, it is most important to model the dynamics of a the radio channel in realistic way. The movement of the nodes also needs to be modelled, however, detailed modelling of the movement patterns has little effect.

Keywords: mobility modelling, channel modelling, wireless networks

Sammanfattning

Vid modellering av taktiska radionät är det viktigt att få med effekter av nodernas mobilitet. I denna rapport jämför vi två mobiltsmodeller, en slumpvandringsmodell och en gruppmobilitetsmodell. Jämfört med slumpvandringsmodellen erbjuder gruppmobilitetsmodellen fler justeringsmöjligheter men har samtidigt en mer komplex struktur.

Utvärdering av en elementär vågform visar att gruppmobilitetsmodellen är mindre utmanande än slumpvandringsmodellen ur kapacitetssynpunkt men att den är mer utmanande sett till andelen trafik som levereras. Gruppmobilitetsmodellen kräver också fler eller längre simuleringar, jämfört med slumpvandringsmodellen för att uppnå samma varians för de studerade metrikerna. Vidare visar utvärderingen att radiokanalen och terrängen har betydligt större påverkan på simuleringsresultaten än nodernas rörelsemönster. Sålunda är det viktigast att modellera radiokanalens dynamik på ett realistiskt sätt. Nodernas rörelser behöver också modelleras emellertid är nyttan av detaljerad modellering av nodernas rörelsemönster begränsad.

Nyckelord: mobilitetsmodellering, kanalmodellering, trådlösa nätverk

Contents

1 Introduction

When modelling tactical radio networks it is important to capture the effects of the nodes' mobility. Common methods to model the nodes mobility is to use either realistic tactical scenarios that describes the movements of the node or mobility models that generate the movements of the nodes. If the degree of realism in the nodes' movement is the only deciding factor, a tactical scenario is normally preferable. However, if other factors such as the development cost for the scenario and the ability to scale network size and mobility also are considered, a mobility model can be a better choice.

There are today a number of mobility models for radio networks with different properties and different pros and cons. For an overview of mobility models see [1] and [2]. The mobility models can be categorized in several different ways. One way, used in [1], is to categorize the models based on their temporal dependency, spatial dependency and ability to handle geographical restrictions. In models with temporal dependency the velocity vector of the nodes will be continuous in time, i.e. no sharp turns or instantaneous accelerations. If the movement of nodes are mutually correlated, the model is classified as a model with spatial dependency. In models that can handle geographical restrictions the movement of the nodes can be restricted by streets or obstacles. The Random Waypoint Model, where the nodes move along straight lines between random positions [3], is an example of a model with none of the above characteristics while the Manhattan Mobility model, where the nodes move in the streets of a town [4], is an example of a model with both temporal dependency and handling of geographical restrictions.

It this report we compare the moments patterns in a tactical scenario with two mobility models, a random walk model [5] and a group mobility model [6], where the models are parameterized based on the movements patterns in the tactical scenario. Both mobility models have temporal dependencies. However, as the names indicate, only the group mobility model have spatial dependency. Furthermore, none of the evaluated models consider geographical restrictions.

In the random walk model all nodes move independently of each other in a square area. If a node hits the boundary of the area it will reflect back like a ball. The design of the group mobility model is based on the assumption that the hierarchic organization of nodes that form this type of network is reflected in the movement patterns of the nodes. The model is inspired by the group mobility model in [7] and the random walk model used here.

In the group mobility model the nodes are structured in a hierarchy of groups. At the lowest level in the hierarchy, the groups consist of individual nodes whereas the groups at higher levels consist of lower levels groups. The movements of the nodes in a group are modelled as a random walk inside a circle that is centred in the centre of the group. Furthermore, the minimum distances between the nodes are limited. The movements of the group's centre is modelled similarly but with a larger radius of the circle and larger minimum distance. The total movement of a node is then calculated as the sum of the node's own movement and the movements of the groups in the hierarchy the nodes belongs to. By changing the parameters in the group mobility model the mobility of the nodes can be varied. Here we present parameter sets for the model

based on a tactical scenario for a battalion.

In the report, we compare the movement patterns in a tactical scenario, the random walk model, and the group mobility model. In the evaluation we focus on how the mobility model affects the performance of a tactical radio network. We consider both how the connectivity of the network is affected by the mobility model and how a basic waveform is affected by the mobility model.

Since the network is influenced mainly by the channel variations caused by the node's mobility, it is important to model the radio channel in a realistic way. The evaluation in this report is based on the stochastic channel model proposed in [8]. However, to illustrate the importance of using a realistic channel model we will also present some result for other channel models.

The report is organized as follows: In chapter 2 the structures of the random walk mobility model and the group mobility model are described. Furthermore, recommended values for the parameters in the mobility models and the method used to select them are then presented. Chapter 3 presents the results of the mobility model comparison and the channel model comparison. Finally, the overall conclusions are presented in section 4.

2 Mobility Models

In this chapter we present the two mobility models that we analyze in the report, in a more formal way. We begin with a description of the random walk model since the group mobility model reuse parts of its structure. We then continue with the description of the group mobility model and the parameter sets that the group mobility model uses.

2.1 Random Walk Model

In the random walk model all nodes moves independently of each other with a constant speed v m/s. The movements are constrained to stay in a fixed area in the form of a square, where the length of the square side is b meters.

Let $\mathbf{r}_{i,p}$ denote the pth chronological position of node i. The positions are assumed to be given in a horizontal plane i.e. $\mathbf{r}_{i,p} = [x_{i,p}, y_{i,p}]$. To each position we associate a velocity vector $\mathbf{v}_{i,p}$ also given in the horizontal plane, for example $\mathbf{v}_{i,p} = (v\cos(\theta_{i,p}), v\sin(\theta_{i,j}))$ where $\theta_{i,p}$ is velocity direction angle for node i at the pth position. Furthermore, the pth position is calculated at sample time t_p, where $t_p = \Delta T(p-1)$ and ΔT is the sample interval.

The initial positions of the nodes are assumed to be uniformly distributed over the square and the initial velocity direction angle for the nodes are assumed to be uniformly distributed over the interval $[0, 2\pi]$, i.e.

$$x_{i,1} \sim \mathrm{U}(0,l)\,,\ y_{i,1} \sim \mathrm{U}(0,b)\,,\ \theta_{i,1} \sim \mathrm{U}(0,2\pi)\,.$$

For each new position $p = 1, 2, \ldots, P$ the position vector, $\mathbf{r}_{i,p}$, is generated as

$$\begin{aligned} x_{i,p+1} &= x_{i,p+1} + \Delta T v\cos(\theta_{i,p}) \\ y_{i,p+1} &= y_{i,p+1} + \Delta T v\sin(\theta_{i,p}) \\ \theta_{i,p+1} &= \theta_{i,p} + \Delta T\omega_{i,p} \end{aligned}$$

where $\omega_{i,p}$ is the angular velocity of the velocity vector $\mathbf{v}_{i,p}$.

The rotation $\omega_{i,p}$ is modelled as a normal distributed process. Furthermore, the autocorrelation function for the process is assumed to be an exponential function. Hence, a sequence of correlated realizations of the process is generated as

$$\omega_{i,p+1} = \begin{cases} \rho\,\omega_{i,p} + \sqrt{1-\rho^2}\Delta T\Omega_p & \text{if } p > 1 \\ \Delta T\Omega_p & \text{if } p = 1 \end{cases}$$

where ρ is a coefficient that determines the statistical dependency between $\omega_{i,p}$ and $\omega_{i,p+1}$ and Ω_p is a Gaussian distributed process with zero mean and variance σ^2 i.e.

$$\Omega_{l,p} \sim \mathrm{N}\left(0, \sigma^2\right)$$

Based on our exponential autocorrelation assumption, we model the coefficient ρ as an exponential function

$$\rho = \exp\left(-\frac{\Delta T}{\Delta\omega}\right)$$

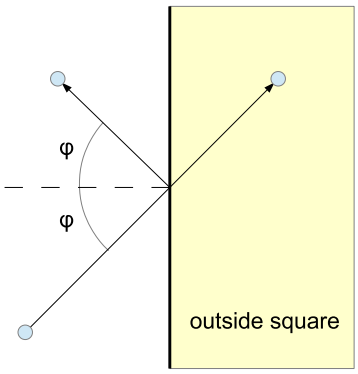

Figure 2.1: Perfectly elastic collision with the side of the square.

Table 2.1: Default parameters for the group mobility model for a network with N nodes.

Parameter	Value	Unit
b	$3500\sqrt{\frac{\pi N}{48}}$	m
v	4.1	m/s
σ	0.071	rad/s
$\Delta\omega$	1.0	s

where $\Delta\omega$ is a time constant.

To limit the movement of the nodes inside the square all positions, $\mathbf{r}_{i,p}$, that falls utside the square are recalculated as if the nodes had bounced in the side of the square. The bounce is modelled as a perfectly elastic collision with the sides of the square, i.e. without loss of speed and with the same angle to the normal of the square side, see Figure 2.1. The velocity direction angle should also be recalculated in the same way so that the velocity vectors, $\mathbf{v}_{i,p}$ are consistent with the movements of the nodes after the bounce.

Parameters for random walk model are presented in Table 2.1.

2.2 Group Mobility Model

In the group mobility model the nodes are assumed to be structured in a hierarchy of groups with L levels where each group at level $l+1$ is divided into G_l subgroups at level l. The highest hierarchical level, L, consist of one group with all nodes, i.e. $G_L = 1$. At the second highest level, $L-1$, the nodes are divided into G_{L-1} subgroups each consisting of N/G_{L-1} nodes, where N is the number of nodes in the model, see Figure 2.2. At hierarchal level l, $l \in \{2, 3, ..., L\}$ each group is further divided into G_l subgroups with $N/(\Pi_{i=l}^{L} G_i)$ nodes. At hierarchical level $l = 1$ all groups contain one node, that is $\Pi_{i=1}^{L} G_i = N$.

We assume that node n belongs to group $g_l(n) = \lceil n/N \times \Pi_{i=l}^{L} G_i \rceil$ at level l.

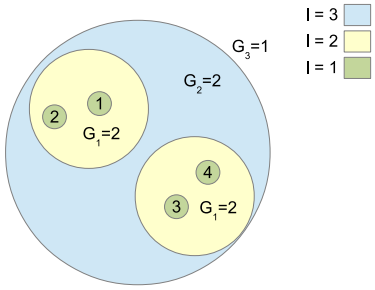

Figure 2.2: Network structure for a network with one main group consisting of two sub groups with two nodes each.

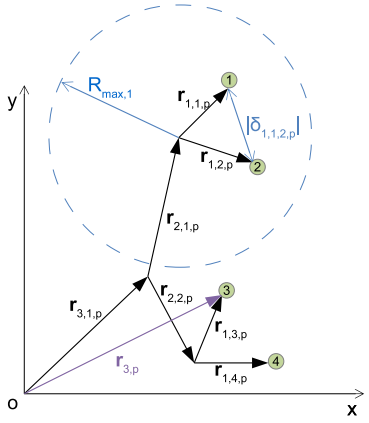

Figure 2.3: Structure of the position vectors $\mathbf{r}_{l,i,p}$ and $\mathbf{r}_{n,p}$ for the network structure in Figure 2.2.

Furthermore, we let the set $\mathcal{F}_n = \{g_1(n), g_2(n), ..., g_L(n)\}$ denote the set of groups node n belongs to at level $1, 2, ..., L$. For example, if $L = 3$, $N = 4$, $G_1 = 2$, $G_2 = 2$, and $G_3 = 1$ the network will consist of one main group consisting of two subgroups with two nodes each. Thus, we get the sets $\mathcal{F}_1 = \{1, 1, 1\}$, $\mathcal{F}_2 = \{2, 1, 1\}$, $\mathcal{F}_3 = \{3, 2, 1\}$, and $\mathcal{F}_4 = \{4, 2, 1\}$, see Figure 2.2.

Let $\mathbf{r}_{l,i,p}$ denote the pth chronological position of group $i \in \mathcal{F}_n$ at level l. The position, $\mathbf{r}_{l,i,p}$, is calculated relative to the position of the group $j \in \mathcal{F}_n$ at level $l + 1$. For level $l = L$ the position is relative the origin of the coordinate system, se Figure 2.3 for an illustration. Furthermore, the pth position is calculated at sample time t_p, where $t_p = \Delta T(p - 1)$ and ΔT is the sample interval. The positions are assumed to be given in a horizontal plane, i.e. $\mathbf{r}_{l,i,p} = [x_{l,i,p}, y_{l,i,p}]$ or $\mathbf{r}_{l,i,p} = [r_{l,i,p} \cos(\theta_{l,i,p}), r_{l,i,p} \sin(\theta_{l,i,p})]$. Thus the pth chronological position, $\mathbf{r}_{n,p}$, for node n can be calculated as

$$\mathbf{r}_{n,p} = \sum_{l=1, i=g_l(n)}^{L} \mathbf{r}_{l,i,p}$$

The initial positions of the groups at level l are assumed to be uniformly distributed over a circle with radius $R_{\max,l}$, i.e.

$$\theta_{l,i,1} \sim \mathrm{U}\left(0, 2\pi\right), \;\; r_{l,i,1} \sim \sqrt{\mathrm{U}\left(0, R_{\max,l}\right)}.$$

Furthermore, we assume that the initial distances between all groups at level l that belongs to the same group at level $l+1$ are larger than $R_{\min,l}$, that is

$$|\boldsymbol{\delta}_{l,i,j,p}| = |\mathbf{r}_{l,i,p} - \mathbf{r}_{l,j,p}| > R_{\min,l} \; \forall i,j \in \mathcal{A}_{l,i}$$

where $\mathcal{A}_{l,i}$ is a set with the groups at level l that belongs to the same group as group i at level $l+1$, i.e.

$$\mathcal{A}_{l,i} = j : g_{l+1}(n) = g_{l+1}(m) \,\text{where}\, g_l(n) = i \,\text{and}\, g_l(m) = j,$$

where n and m are nodes. Thus, for the example in Figure 2.2 we get groups $\mathcal{A}_{1,1} = \{2\}$, $\mathcal{A}_{1,2} = \{1\}$, $\mathcal{A}_{1,3} = \{4\}$, and $\mathcal{A}_{1,4} = \{3\}$ for $L = 1$; $\mathcal{A}_{2,1} = \{2\}$ and $\mathcal{A}_{2,2} = \{1\}$ for $L = 2$; and $\mathcal{A}_{3,1} = \{\}$ for $L = 3$.

To each position $\mathbf{r}_{l,i,p}$ we associate a velocity vector, $\mathbf{v}_{l,i,p}$ also given in the horizontal plane, for example $\mathbf{v}_{l,i,p} = \left(v_{l,i,p}\cos\left(\phi_{l,i,p}\right), \, v_{l,i,p}\sin\left(\phi_{l,i,p}\right)\right)$. The initial velocity for all groups at level l is set to v_l while the directions $\phi_{l,i,1}$ are assumed to be uniformly distributed over the interval $[0, 2]$, i.e.

$$\phi_{l,i,1} \sim \mathrm{U}\left(0, 2\pi\right).$$

For each new position $p = 1, 2, ..., P$ the velocity vector $\mathbf{v}_{l,i,p}$ and the position vector $\mathbf{r}_{l,i,p}$ are generated as

$$\begin{aligned}
\mathbf{v}_{l,i,p+1} &= \mathbf{R}_{l,i,p}\left\{\mathbf{v}_{l,i,p} + \Delta T \frac{\mathbf{F_T}\left(\mathbf{r}_{l,i,p}\right)}{m}\right\} \\
\mathbf{r}_{l,i,p+1} &= \mathbf{r}_{l,i,p+} + \Delta T \mathbf{v}_{l,i,p}
\end{aligned}$$

where $\mathbf{R}_{l,i,p}$ is a rotation matrix which models the random walk behavior of the model, $m = 1$ kg is a unit mass, and $\mathbf{F_T}$ a force that controls the movement of the groups. The rotation matrix $\mathbf{R}_{l,i,p}$ is structured as

$$\mathbf{R}_{l,i,p} = \begin{bmatrix} \cos\left(\omega_{l,i,p}\right) & -\sin\left(\omega_{l,i,p}\right) \\ \sin\left(\omega_{l,i,p}\right) & \cos\left(\omega_{l,i,p}\right) \end{bmatrix}.$$

The rotation $\omega_{l,i,p}$ is modelled as a normal distributed process. Furthermore, the autocorrelation function for the process is assumed to be an exponential function. Hence, a sequence of correlated realizations of the process is generated as

$$\omega_{l,i,p+1} = \begin{cases} \rho_l \omega_{l,i,p} + \sqrt{1-\rho_l^2}\Delta T \Omega_{l,p} & \text{if}\, p > 1 \\ \Delta T \Omega_{l,p} & \text{if}\, p = 1 \end{cases}$$

where ρ_l is a coefficient that determines the statistical dependency between $\omega_{l,i,p}$ and $\omega_{l,i,p+1}$ and $\Omega_{l,p}$ is a Gaussian distributed process with zeros mean and variance σ_l^2 at level l i.e.

$$\Omega_{l,p} \sim \mathrm{N}\left(0, \sigma_l^2\right)$$

Based on our exponential autocorrelation assumption, we model the coefficient ρ_l as an exponential function

$$\rho_l = \exp\left(-\frac{\Delta T}{\Delta \omega_l}\right)$$

where $\Delta\omega_l$ is a time constant.

The force $\mathbf{F_T}$ has three components: a force that limits the movement of the groups into a circle around the group centre, $\mathbf{F_b}\left(\mathbf{r}_{l,i,p}\right)$; a force that limits the minimum distance between the groups, $\mathbf{F_d}\left(\mathbf{r}_{l,i,p}\right)$; and a force that controls the velocity of the groups, $\mathbf{F_a}\left(\mathbf{r}_{l,i,p}\right)$. The total force $\mathbf{F_T}$ is then calculated as

$$\mathbf{F_T} = \mathbf{F_b} + \mathbf{F_d} + \mathbf{F_a}\,.$$

The force $\mathbf{F_b}\left(\mathbf{r}_{l,i,p}\right)$, that limits the movement of the groups into a circle, is modeled as an ideal spring pulling groups towards the center of the group

$$\mathbf{F_b}\left(\mathbf{r}_{l,i,p}\right) = \begin{cases} -k_{\max,l}\hat{\mathbf{r}}_{l,i,p}\left(|\mathbf{r}_{l,i,p}| - R_{\max,l}\right) & \text{if } |\mathbf{r}_{l,i,p}| > R_{\max,l} \\ \mathbf{0} & \text{if } |\mathbf{r}_{l,i,p}| \leq R_{\max,l} \end{cases}$$

where $k_{\max,l}$ is a spring coefficient at level l, $\hat{\mathbf{r}}_{l,i,p} = \mathbf{r}_{l,i,p}/|\mathbf{r}_{l,i,p}|$ is a unit vector, and $R_{\max,l}$ the target radius for level l. The spring coefficient $k_{\max,l}$ is modeled as ideal spring pushing groups apart

$$k_{\max,l} = \frac{m v_l^2}{R_{\max,l}^2} \times \alpha$$

where v_l is the target velocity of groups at level l, and α a scaling factor that controls how far outside the circle the nodes can be. A high value of α means that nodes outside $R_{\max,l}$ are pushed back inside $R_{\max,l}$ faster. The force $\mathbf{F_d}\left(\mathbf{r}_{l,i,p}\right)$, that limits the minimum distance between the groups, is modeled as

$$\mathbf{F_d}\left(\mathbf{r}_{l,i,p}\right) = \sum_{\forall j \in \mathcal{A}_{l,i}} \acute{\mathbf{F}}_{\mathbf{d}}\left(\boldsymbol{\delta}_{l,i,j,p}\right)$$

where $\boldsymbol{\delta}_{l,i,j,p} = \mathbf{r}_{l,i,p} - \mathbf{r}_{l,j,p}$ is the distance vector between group i and j and $\acute{\mathbf{F}}_{\mathbf{d}}\left(\mathbf{r}_{l,i,p}\right)$ is modelled as

$$\acute{\mathbf{F}}_{\mathbf{d}}\left(\mathbf{r}_{l,i,p}\right) = \begin{cases} k_{\min,l}\hat{\boldsymbol{\delta}}_{l,i,j,p}\left(R_{\min,l} - |\boldsymbol{\delta}_{l,i,j,p}|\right) & \text{if } |\boldsymbol{\delta}_{l,i,j,p}| < R_{\min,l} \\ \mathbf{0} & \text{if } |\boldsymbol{\delta}_{l,i,j,p}| \geq R_{\min,l} \end{cases}$$

where $k_{\min,l}$ is a spring coefficient at level l, $\hat{\boldsymbol{\delta}}_{l,i,j,p} = \boldsymbol{\delta}_{l,i,j,p}/\left|\boldsymbol{\delta}_{l,i,j,p}\right|$ is a unit vector and $R_{\min,l}$ the minimum group distance for level l. The spring coefficient $k_{\min,l}$ is modeled as

$$k_{\min,l} = \frac{m v_l^2}{R_{\min,l}^2} \times \alpha$$

Table 2.2: Default parameters for the group mobility model for a network with 48 nodes.

Parameter	48 nodes	Unit
L	4	-
$G_l, \{G_1, G_2, G_3, G_4\}$	$\{3, 4, 4, 1\}$	-
$R_{\max,l}$	$\{165, 1000, 3500, \inf\}$	m
$R_{\min,l}$	$\{35, 200, 1600, 0\}$	m
v_l	$\{0.5, 2.3, 2.3, 3.2\}$	m/s
ΔT	0.01	s
σ_l	$\{0.063, 0.063, 0.047, 0\}$	rad/s
$\Delta\omega_l \, \forall \, l$	1.0	s
α	32	-
$a_{\max}$	0.05	m/s^2

where v_l is the target velocity of groups at level l and α is a scaling factor. Finally, the force $\mathbf{F_a}\left(\mathbf{r}_{l,i,p}\right)$, that controls the velocity of the groups, is modeled as

$$\mathbf{F_a}\left(\mathbf{r}_{l,i,p}\right) = \begin{cases} a_{\max}\hat{\mathbf{v}}_{l,i,p} & \text{if } |\mathbf{v}_{l,i,p}| < v_l \\ \mathbf{0} & \text{if } |\mathbf{v}_{l,i,p}\,| = v_l \\ -a_{\max}\hat{\mathbf{v}}_{l,i,p} & \text{if } |\mathbf{v}_{l,i,p}\,| > v_l \end{cases}$$

where $a_{\max}$ is the maximum acceleration of a group and v_l is the target velocity of groups at level l.

2.3 Group Mobility Model Parameters

Parameters for the group mobility model for networks with 48 nodes are presented in Table 2.2. The parameters for the network with 48 nodes are based on the parameters used in [5] and the movement patterns in the tactical scenario in Lomben in [9]. The parameters for the 72 and 140 nodes networks, presented in Table 2.3, are based on the 48 node network and only differ in terms of the group structure and the circle radius. The group structure is based on the structure of the units in the Lomben scenario and the symmetry requirements of the mobility model. The radiuses are adjusted so that the node density is equal for all network sizes.

The parameters estimated for the network with 48 nodes is based on a subset of the Lomben scenario where all used nodes move in groups in the terrain. The subset consists of the movement patterns for node 13-24, 37-48, 61-72 and 85-96 between time $t = 5500$ s and $t = 6500$ s. Thus, the used scenario consist of nodes from one battalion, forming four companies, each consisting of four groups of three units, i.e. $L = 4$ and $\{G_1, G_2, G_3, G_4\} = \{3, 4, 4, 1\}$.

At the highest level, $l = L$ in the model, the parameters $R_{\max,l}$ and $R_{\min,l}$ are assumed to be set to infinity and zero, respectively. The speed v_L is estimated as the average speed of the center of gravity for all nodes in the network. To estimate the speed at at level $L - 1$ the coordinates are first transformed to the relative coordinate system of level $L - 1$ by for each time t removing the center of gravity at level L. The

Table 2.3: Default parameters for the group mobility model for networks with 72 and 140 nodes.

Parameter	72 nodes	140 nodes	Unit
L	4	4	-
$G_l, \{G_1, G_2, G_3, G_4\}$	$\{3, 4, 6, 1\}$	$\{4, 5, 7, 1\}$	-
$R_{\max,l}$	$\{165, 1000, 4300, \inf\}$	$\{190, 1300, 6000, \inf\}$	m
$R_{\min,l}$	$\{35, 200, 1600, 0\}$	$\{35, 200, 1600, 0\}$	m
v_l	$\{0.5, 2.3, 2.3, 3.2\}$	$\{0.5, 2.3, 2.3, 3.2\}$	m/s
ΔT	0.01	0.01	s
σ_l	$\{0.063, 0.063, 0.047, 0\}$	$\{0.063, 0.063, 0.047, 0\}$	rad/s
$\Delta\omega_l \, \forall \, l$	1.0	1.0	s
α	32	32	-
$a_{\max}$	0.05	0.05	m/s^2

speed is then estimated as the average speed of the center of gravity for the groups at level $L - 1$.

To estimate $R_{\max,L-1}$ and $R_{\min,L-1}$ we estimate the distance to origin distribution and intergroup distance distribution, respectively. The distance to origin distribution models the distance between groups center of gravity and the origin of the relative coordinate system. The intergroup distance distribution models the distance between different groups center of gravity. The parameter $R_{\max,L-1}$ is estimated as the 95% percentile of the distance to origin distribution whereas parameter $R_{\min,L-1}$ is estimated as the 5% of percentile of the intergroup distance distribution. The process is then repeated for all levels l until all parameters are estimated.

The parameters that models the random walk characteristics of the model, σ_l, and $\Delta\omega_l$, are based on the corresponding parameters for the random walk model in section 2.1. The time ΔT, the constant α and the acceleration $a_{\max}$ are design parameters. The time ΔT controls the stability of the differential equations that describes the model whereas α and $a_{\max}$ control the movements of the nodes.

3 Model Comparison

In this chapter we compare the group mobility model, the random walk model and movement patterns from the tactical scenario . We begin by comparing the movement patterns, we then continue by comparing how the connectivity of the networks are affected by the mobility model. Furthermore, we analyze how the used metrics varies for different realizations of the mobility models and how the channel model affects the results. Finally, we compare how a basic waveform is affected by the mobility model.

In all comparisons the speed of the nodes in the random walk model is equal to the mean speed of the nodes in the group mobility model. Furthermore, the node density in the random walk model is equal to the node density inside the level $L = 4$ circle in the group mobility model. All metrics are presented for different values of the maximum path loss, $L_{b,\max}$, that the system can establish a link over. Unless otherwise stated, we use stochastic channel model in [8] to calculated the path loss between the nodes. Furthermore, we set the carrier frequency to 300 MHz.

3.1 Movement Patterns

In Figure 3.1 the movement patterns from the tactical scenario used to select the parameters in the model in section 2.3 are compared with movement patterns generated with the group mobility model and the random walk model used in [5]. All networks consist of 48 nodes. The figure shows that the movement patterns generated by the group mobility model have similar character as the movement patterns in the tactical reference scenario, whereas the movement patterns generated by the random walk model exhibit relatively different character.

3.2 Network Connectivity

To investigate how different mobility models influence the structure of the network we consider two metrics, the connectivity of the network and the neighbor change rate. The connectivity is defined as the average number of neighbors a node has divided by the maximum number of neighbors. Thus, if the connectivity if 0.5 in a network with 48 nodes the nodes will in average have $(48-1)\times 0.5 = 23.5$ neighbors. The neighbor change rate is measured as the average number of new neighbors a node detects per second. Note that on average this is the same as the number of lost neighbors. In the evaluation we consider networks with 48, and 72 nodes where the movement patterns are generated by the mobility models. For each network size and mobility model, 11 realizations are generated, each with a duration of 3000 s. We also include results for the tactical scenario with 48 nodes, note that the duration of the tactical scenario is 1000 s.

The network connectivity for the flat rural area and the hilly rural area is presented in Figure 3.2(a) and Figure 3.2(b), respectively. When $L_{b,\max}$ increases, the number of available neighbors will also increase and for high values of $L_{b,\max}$ the networks in the flat rural areas are almost one hop networks for the networks in Figure 3.2(a). Due

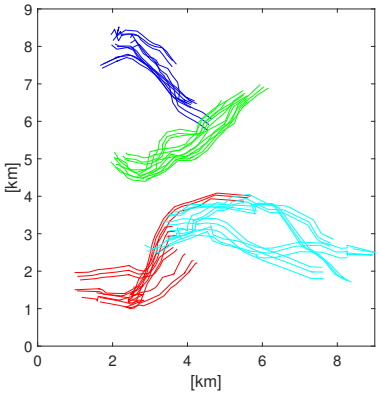

(a) Tactical scenario in Lomben.

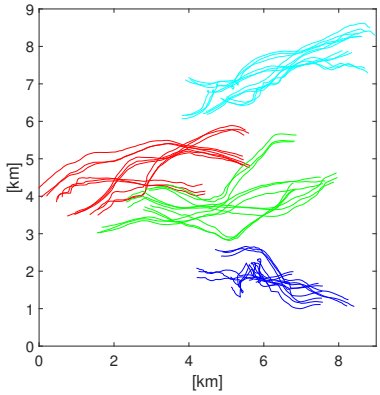

(b) Group mobility model.

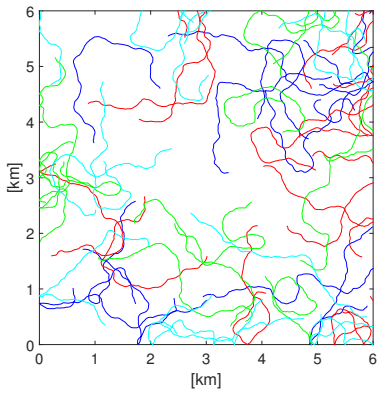

(c) Random walk model.

Figure 3.1: Illustration of the movements of the nodes for a scenario with 48 nodes. In 3.1(a) and 3.1(b) all nodes move to the right. Nodes with the same color belong to the same group at level $L - 1 = 3$, i.e. the same company.

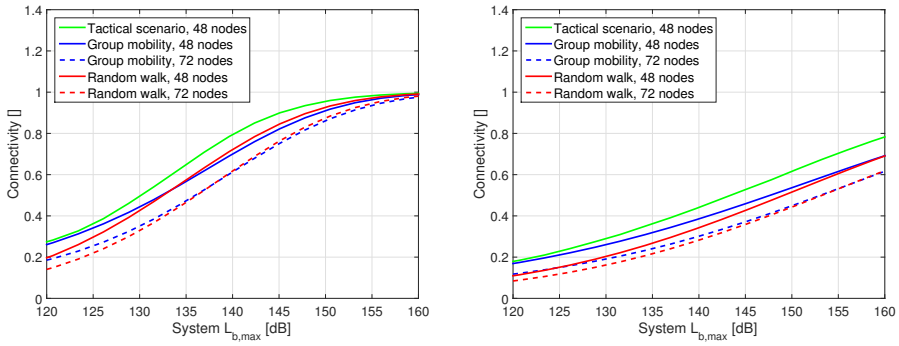

(a) Flat rural area.

(b) Hilly rural area.

Figure 3.2: Network connectivity as function of different $L_{b,\max}$.

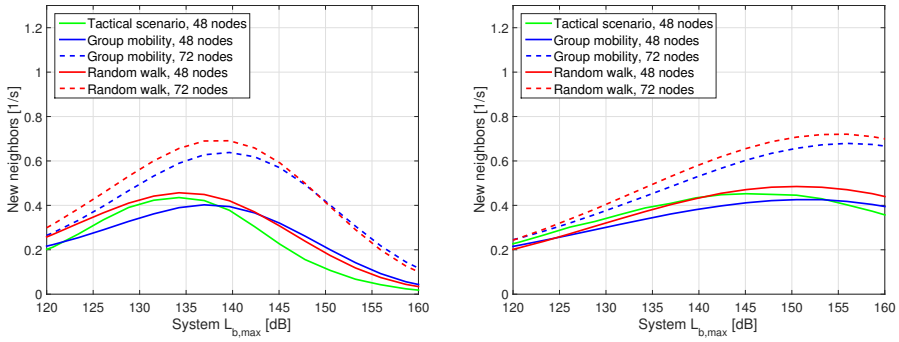

(a) Flat rural area.

(b) Hilly rural area.

Figure 3.3: Neighbor change rate as function of different $L_{b,\max}$.

to a higher distance dependent path loss, the connectivity is lower in the hilly rural area in Figure 3.2(b) for the same link threshold $L_{b,\max}$.

For a given terrain and network size the differences between the models are relatively small. The biggest difference is for low values of $L_{b,\max}$ where the connectivity is higher for the group mobility model than for the random walk model. Compared to the tactical scenario both mobility models show a lower connectivity for the networks with 48 nodes.

The neighbor change rate for the flat rural area and the hilly rural area is shown in Figure 3.3(a) and Figure 3.3(b), respectively. For a given network size the difference in neighbor change rate between the models is small. The increase in the neighbor change rate when the network size increases is explained by the fact that there exists more potential links in a network with more nodes. In the same way the neighbor change rate will increase with increasing $L_{b,\max}$ until the increase in links that are stable starts to dominate. The maximum of the curves in the figure will occur at the $L_{b,\max}$ when that happens.

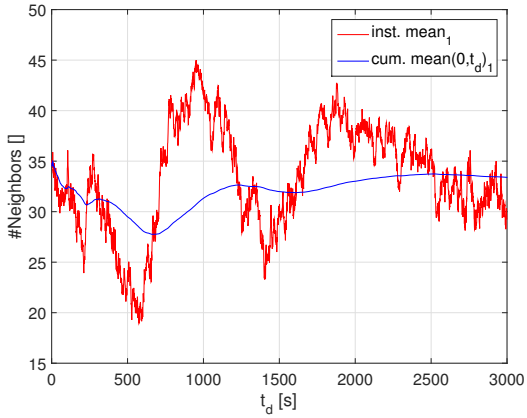

Figure 3.4: Instantaneous mean and cumulative mean number of neighbors of the first realization as a function of the scenario duration t_d for $L_{b,\max} = 140$ dB.

3.3 Metric Variance

A key issue when using a stochastic mobility model to evaluate the performance of a waveform is how much the simulation results differ for different realizations of the mobility model. In this section we will therefore analyse the variance of some measures for a set of realizations of the used mobility models.

Figure 3.4 shows the instantaneous number of neighbors, denoted with inst. mean, and the cumulative average number of neighbors, dentoed with cum. mean, for one realization of the random walk model. The path-gains are calculated with the stochastic channel model configured for the flat rural terrain. The cumulative average number of neighbors can be seen as the average number of neighbours if the scenario duration was t seconds. As expected, the cumulative average stabilize more and more as the scenario length t_d increases. In Figure 3.5 the cumulative average numbers of neighbours is shown for 11 realizations of the model used in Figure 3.4. For each t_d we have also calculated the average value of the cumulative average. The figure shows that the spread between different realizations is noticeable for low values of t_d, i.e. short scenario length. As the scenario length increase the spread decrease. However, for scenario durations t_d above 1000 seconds the decrease is slow and for a scenario length of $t_d = 3000$ seconds the spread is still not negligible.

As a measure of the spread the variance of the cumulative average number of neighbors is shown for the flat rural area and the hilly rural area in Figure 3.6(a) and Figure 3.6(b), respectively. For low values of t_d , that is short scenario lengths, the variance estimates fluctuates. As scenario length t_d increases the variance estimates stabilize and slowly decrease. However, the decrease is relatively slow and even with a scenario length $t_d = 3000$ s the variance is non negligible.

For scenario lengths around and above $t_d = 1000$ there is a larger variance between different realizations of the group mobility model than between realizations of the random walk model in the flat rural terrain. The same applies to networks with 48

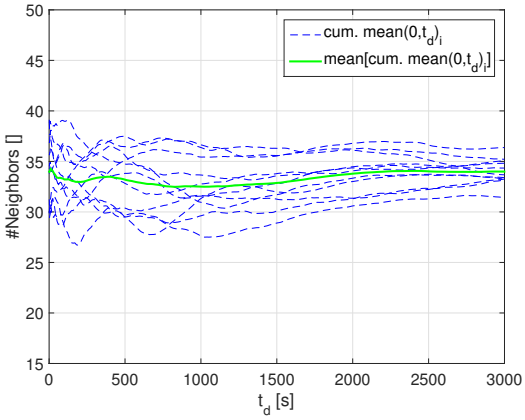

Figure 3.5: Estimated cumulative average number of neighbors for realizations $i \in \{1, 2, \ldots, 11\}$ of the group mobility model as a function of the scenario duration t_d for $L_{b,\max} = 140$ dB.

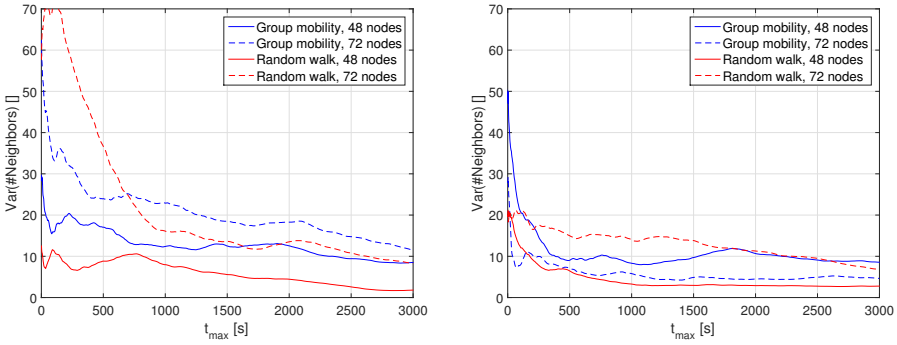

(a) Flat rural area.

(b) Hilly rural area.

Figure 3.6: Estimated variance of the cumulative average number of neighbors as a function of the scenario length t_d for $L_{b,\max} = 140$ dB.

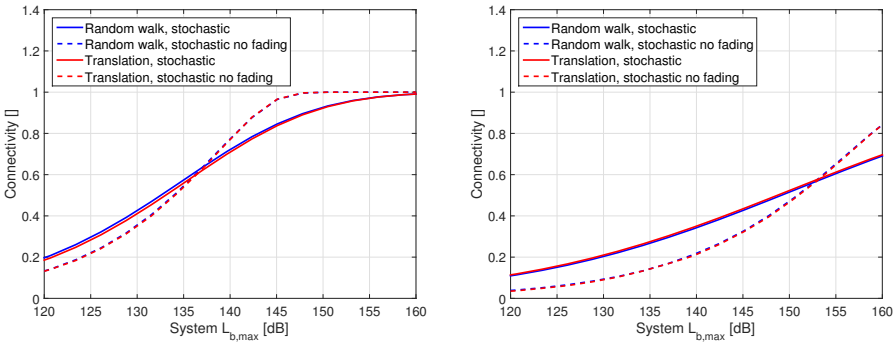

(a) Flat rural area.

(b) Hilly rural area.

Figure 3.7: Network connectivity as function of different $L_{b,\max}$.

nodes in the hilly rural terrain. The situation is the reverse for the larger networks in the hilly terrain where the variance of the group mobility model decreases when the network size increases. However, the comparison of the synthetic channel model with a uniform geometrical theory of diffraction (UTD) model by Holm [10] in appendix A indicates that the last result may be due to deficiencies in the used channel model.

3.4 Radio Channel Modelling

The mobility of the nodes will primarily affect the radio network through the dynamics of the radio channel. Thus, it is important to model the dynamics of the radio channel in a realistic way. To illustrate the importance of radio channel modelling we compare two different channel models, the stochastic channel model and a channel model with only the distance dependent part in the stochastic channel model, denoted as *stochastic no fading*.

To further illustrate the influence of channel the model, two mobility models are considered, the random walk model and a simplified random walk model, denoted as the *translation* model. In the translation model the distribution of the nodes' start position is the same as in the random walk model. However, instead of making a random walk the nodes original positions are translated with the same speed as the nodes move in the random walk model, but in a constant direction. The speed of the nodes in the translation model will thus be equal to the speed of the nodes in the random walk model while the spacing between the nodes will be constant. All results in this section are based on 11 realizations of the mobility models, each with a duration of 3000 s.

The network connectivity of the four cases above is shown in Figure 3.7(a) and Figure 3.7(b) for the flat rural area and the hilly rural area, respectively. Figure 3.7 shows that for a specific channel model the difference between the random walk model and the translation model very is small. For low values of $L_{b,\max}$ the stochastic non fading channel model results in lower connectivity than the stochastic model. This is

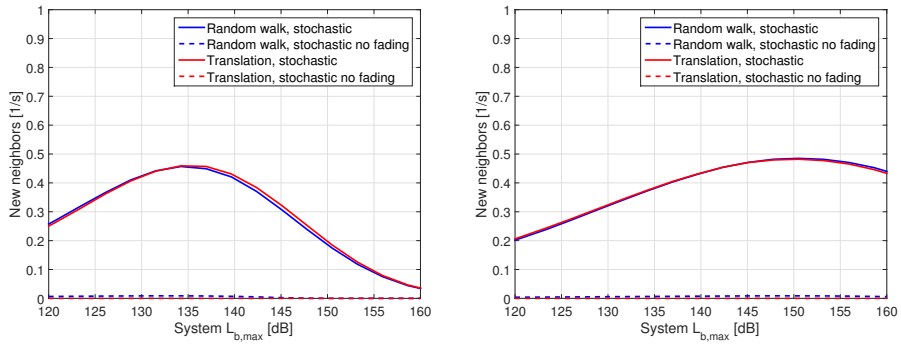

(a) Flat rural area.

(b) Hilly rural area.

Figure 3.8: Neighbor change rate as function of different $L_{b,\max}$.

a result of there being more potential links that can become usable than links that are usable in a network with low connectivity. Thus, the fading will result in more new links than lost links. For high values of $L_{b,\max}$ the process is the reverse.

The connectivity for the hilly terrain, in Figure 3.7(b), is generally lower than the connectivity for the flat rural terrain, in Figure 3.7(a), due to a higher distance dependant path loss in the hilly area. Furthermore we can see that the difference between the channel models is higher in the hilly rural terrain due to stronger large scale fading.

The neighbor change rate of the four cases for the flat rural area and the hilly rural area is shown in Figure 3.8(a) and Figure 3.8(b), respectively. As expected, the neighbor change rate is zero for the translation mobility model in combination with the non-fading channel, since the spacing between the nodes is constant. However, the neighbor change rate is also close to zero for the random walk model in combination with the non-fading channel model. For the fading channel model the difference is small between the random walk model and the translation model. In the hilly terrain the maximum of the neighbor change rate is reached for a higher system threshold $L_{b,\max}$ than in the flat rural terrain, due to a higher distance dependant path loss. However, the overall shape of the curves is similar to the curves for the flat rural terrain but shifted.

The results indicate that the dynamics of the radio channel depends more on the radio channel model than the mobility model. Thus, it is very important that the radio channel model capture the dynamics of the radio channel in a realistic way.

3.5 Waveform Simulations

To exemplify how the mobility models may affect the performance of a waveform a basic waveform is evaluated. In the evaluation the user traffic is modelled as broadcast transmissions of packets, i.e. all packets are sent to all nodes. A basic time-division multiple access MAC protocol, with equal static sharing of time slots, is used for the simulations. To route the packets in the network, we use the Multi-Point-Relay (MPR) method according to the Simplified Multicast Forwarding (SMF) framework [11], and

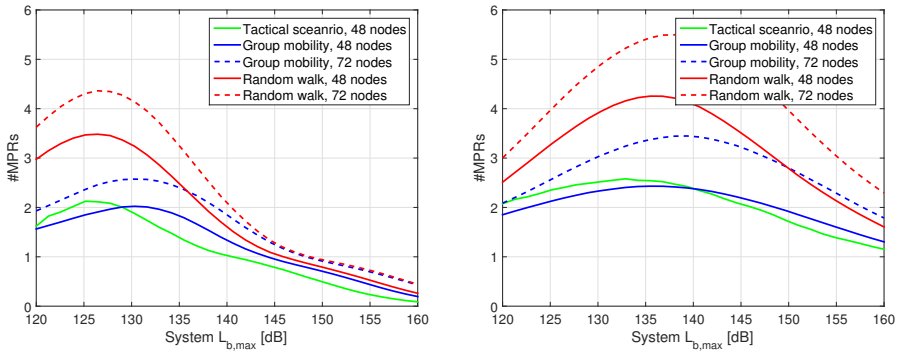

(a) Flat rural area.

(b) Hilly rural area.

Figure 3.9: Average number of MPRs a node selects.

the MPR selection mechanisms in Optimized Link State Routing protocol (OLSR) [12]. Both user and overhead traffic is transmitted in the network. However, the amount of user traffic is moderate since it is only used to probe the network and generate performance measures. For a more detailed description of the waveform see [5].

Four different metrics are considered: the average number of MPR nodes a node selects, the MPR change rate, the average number of retransmission of a packet, and delivery ratio for the user traffic. The MPR change rate is measured as the average number of new MPR nodes a node selects per second and the delivery ratio is measured as the fraction of user packets that reaches their destinations. In the evaluation we consider networks with 48 and 72 nodes generated by the mobility models. We also include results for the tactical scenario with 48 nodes. The results are based on 11 realization with a duration of 1000 s of for each configuration.

The number of MPR nodes a node selects in the flat rural area and in the hilly rural area is shown in Figure 3.9(a) and Figure 3.9(b), respectively. For low values of $L_{b,\max}$ the number of MPRs increases when $L_{b,\max}$ increases, since the number of two hop-neighbors that the MPRs shall cover is increasing. However, for higher values of $L_{b,\max}$ the main effect of increasing $L_{b,\max}$ is that the number of MPR required to connect the network decreases since more and more of the two-hop neighbors becomes one hop neighbors. The higher number of MPRs for the random walk models indicates that the structure of these networks are more challenging.

The MPR change rate in the flat rural area and in the hilly rural area are shown in Figure 3.10(a) and Figure 3.10(b), respectively. For a given network size the MPR change rate is consistently higher for the random walk model than for the group mobility model while the tactical scenario is relative close to the group mobility model. The MPR change rate is both influenced by the number of MPRs a node select and the neighbor change rate. Thus, the results for the MPR change can be seen as a combination of the these results, see Figure 3.9 and Figure 3.3, respectively

The average number of retransmission in the flat rural area and in the hilly rural area are shown in Figure 3.11(a) and Figure 3.11(b), respectively. The average number of retransmissions is closely linked to the amount input traffic that the network handle.

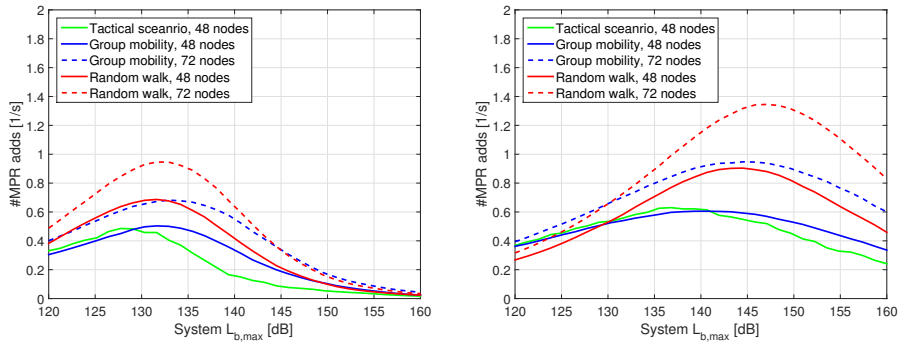

(a) Flat rural area.

(b) Hilly rural area.

Figure 3.10: Average number of MPR additions for a node per second.

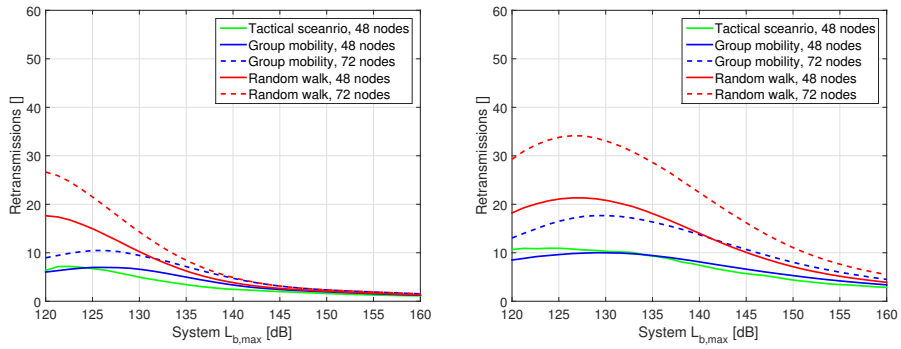

(a) Flat rural area.

(b) Hilly rural area.

Figure 3.11: Average number of retransmissions for a data packet as a function of as function of $L_{b,\max}$.

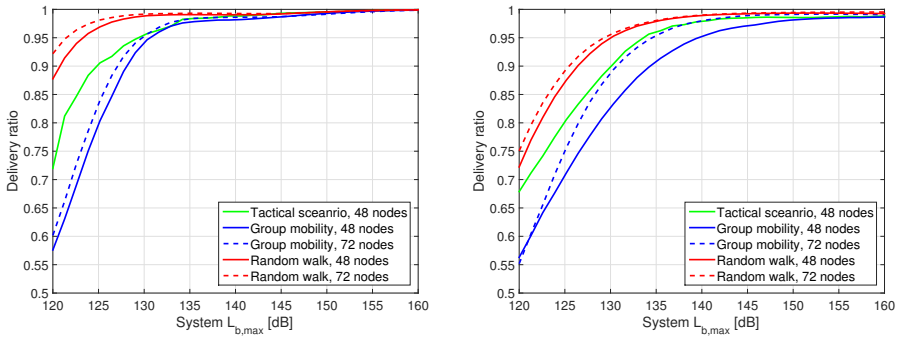

(a) Flat rural area.

(b) Hilly rural area.

Figure 3.12: Delivery ratio for different mobility models.

Basically, a doubling in the number of retransmissions would lead to the amount of input traffic the network can handle being halved. The number of retransmissions is also closely linked to the number of MPRs in the network. However, since not all MPRs need to retransmit a packet according to the SMF framework [11] the number of retransmissions do not need to be equal to the number of MPRs in the network.

The difference in number of retransmissions between the mobility models is small for networks with high connectivity. However, for networks with lower connectivity the random walk model requires more retransmissions than the group mobility model. Thus, the capacity for the networks generated by the random walk model could be expected to be lower than the capacity of the networks generated with the group mobility model.

The delivery ratio in the flat rural area and in the hilly rural area is shown in Figure 3.12(a) and Figure 3.12(b), respectively. The mutual ranking of the models is equal for the different terrain areas. However, a higher $L_{b,\max}$ is required to obtain the same delivery ratio in the hilly rural area compared to the flat rural area, due to the higher path loss in the hilly rural area. For low values of $L_{b,\max}$ the delivery ratio increases fast with increasing $L_{b,\max}$ which indicate the networks is not fully connected, that is, all nodes cannot be reached. If we compare Figure 3.12 and Figure 3.2 for low values of $L_{b,\max}$ we can also see that the random walk model has a higher delivery ratio than the group mobility model for a given number of neighbors. From delivery ratio perspective the random walk model thus seems less challenging than the group mobility model.

4 Conclusions

In this report a group mobility model is evaluated against a random walk model without groups and a tactical reference scenario. The evaluation shows that the group mobility model generates movement patterns with similar character as the movement patterns in a tactical reference scenario whereas the movement pattern generated by the random walk model exhibits relatively different character. Compared to the random walk model, the group model offers more adjustment options but has a more complex model structure. Furthermore, the group model requires more or longer simulations compared to the random walk model to obtain the same variance the evaluated metrics.

In terms of connectivity and link change rate the difference between the mobility models is small. Evaluation of some likely functions of a waveform shows that the networks generated by the group mobility model is less challenging than networks generated by the random walk model in terms of available capacity but more challenging in terms of delivery ratio. However, generalizations to other waveforms of the results from the simulations should be made with caution.

The evaluation also shows that the radio channel and the used terrain area usually have much more effect on the simulation result than the movement patterns of the nodes. Thus, it is most important to model the dynamics of a the radio channel in realistic way. The movement of the nodes also needs to be modelled, however, detailed modelling of the movement patterns has little effect.

A Evaluation of the Stochastic Channel Model

The result in this report are based on the stochastic channel model proposed and evaluated in [8]. In [8] the stochastic channel model is compared to a uniform geometrical theory of diffraction (UTD) model by Holm [10] in the propagation library DetVag-90® [13] for networks where the mobility is generated by the random walk model.

Since a large portion of the simulations in this report are based on the group mobility model we choose here to include a small comparisons of results obtained with the random walk model and the group mobility model for the channel models used in original evaluation. In the evaluation we use 11 realizations of networks with 48 nodes and 11 realizations of networks 72 nodes, each with a duration of 3000 s. Furthermore, we use a carrier frequency of 300 MHz and consider two types of terrain, a flat rural area and a hilly rural area.

In Figure A.1 and Figure A.2 we present the connectivity for 48 and 72 node networks, respectively. For the random walk model the difference in connectivity between the stochastic channel model and UTD model is relatively small for both terrain areas and both network sizes. The same applies to group mobility model in the hilly rural area. However, in the flat rural area the difference in connectivity is larger.

The neighbor change rate is for 48 and 72 node networks is shown in Figure A.3 and Figure A.4, respectively. Compared to the connectivity in Figure A.1 the difference between the channel models is larger for the the neighbor change rate. The difference the between the channel models is most notable for the group mobility model in the flat rural area where the neighbor change rate is significantly lower for the stochastic channel model.

The variance of the cumulative average number of neighbors for 48 and 72 node networks is shown in Figure A.5 and Figure A.6, respectively. For the smaller networks with 48 nodes the variance is higher for the group mobility model than for the random walk model regardless of channel model and terrain area. For the larger networks with 72 nodes the trend seems to be the same for longer scenario durations. However, for shorter durations the variance for the random walk mobility model in combination with the stochastic channel model seems to generate scenarios with relatively high variance.

Note that the used configuration of the group mobility model does not limit the movement of the nodes to a limited area. Thus, the geographical area the nodes move around in will increase with the scenario duration. For UTD model this means variation between different realizations will increase with time since the terrain data the UTD model is using to calculate the path loss varies more and more as the geographical area increases. The effect of this can be seen in Figure A.5 and Figure A.6, variation between different realizations will thereby increase.

The general trend that the difference between the channel models is larger for the group mobility model than for the random walk model might be an effect of that the parameters for the stochastic channel model are estimated on scenarios generated by the random walk model. Thus it is possible that estimation of new parameters for the stochastic channel model on scenarios generated by the group mobility model would

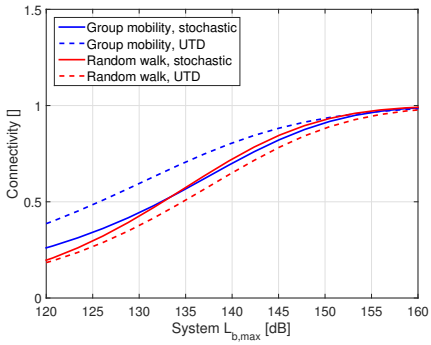

(a) Flat rural area.

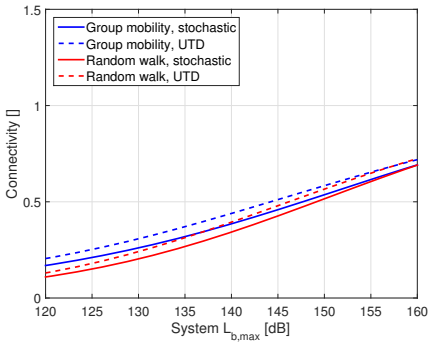

(b) Hilly rural area.

Figure A.1: Network connectivity as function of different $L_{b,\max}$ for networks with 48 nodes.

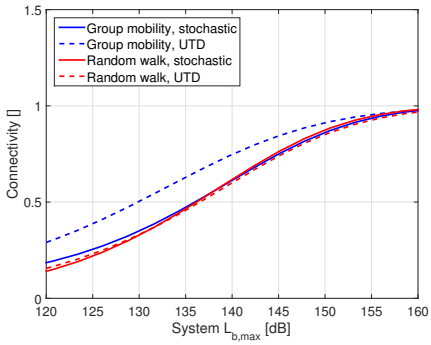

(a) Flat rural area.

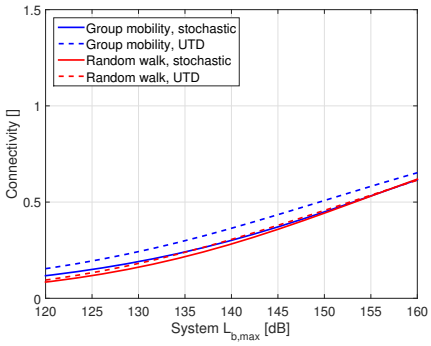

(b) Hilly rural area.

Figure A.2: Network connectivity as function of different $L_{b,\max}$ for networks with 72 nodes.

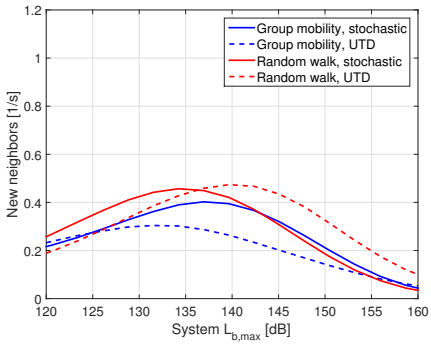

(a) Flat rural area.

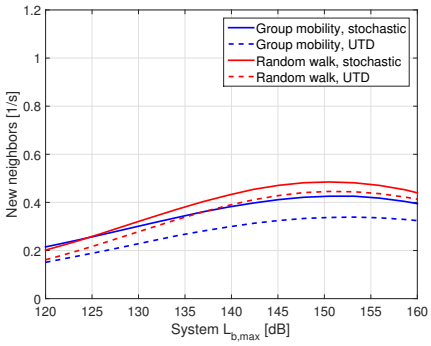

(b) Hilly rural area.

Figure A.3: Neighbor change rate as function of different $L_{b,\max}$ for networks with 72 nodes.

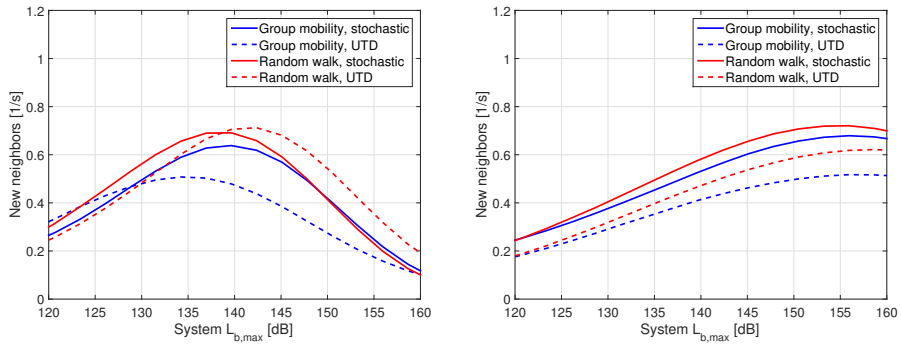

(a) Flat rural area. (b) Hilly rural area.

Figure A.4: Neighbor change rate as function of different $L_{b,\max}$ for networks with 72 nodes.

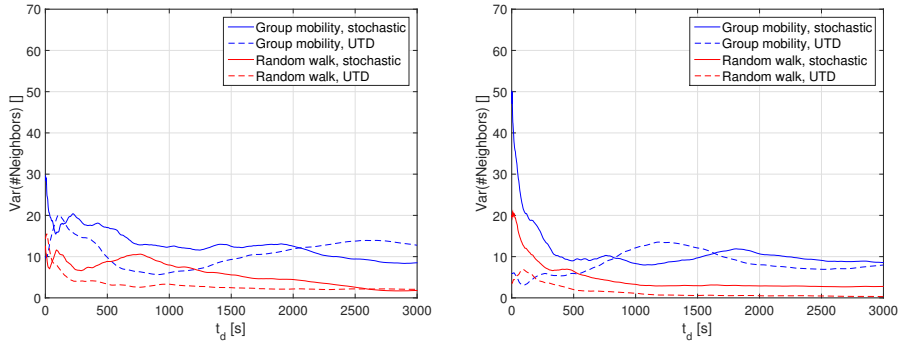

(a) Flat rural area. (b) Hilly rural area.

Figure A.5: Estimated variance of the cumulative average number of neighbors as a function of the scenario length t_d for networks with 48 nodes and $L_{b,\max} = 140$ dB.

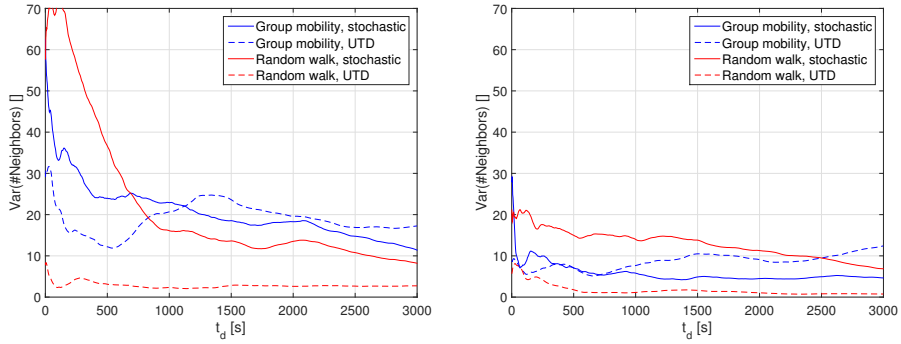

(a) Flat rural area. (b) Hilly rural area.

Figure A.6: Estimated variance of the cumulative average number of neighbors as a function of the scenario length t_d for networks with 72 nodes and$L_{b,\max} = 140$ dB.

decrease the difference between the stochastic channel model and the UTD model for the group mobility model.

References

[1] N. Aschenbruck, E. Gerhards-Padilla, , and P. Martini, “A survey on mobility models for performance analysis in tactical mobile networks,” *Journal of Telecommunications and Information Technology*, no. 2, pp. 54–61, 2008.

[2] N. Aschenbruck, E. Gerhards-Padilla, and P. Martini, “Modeling mobility in disaster area scenarios,” *Performance Evaluation*, vol. 66, no. 12, pp. 773–790, 2009, performance Evaluation of Wireless Ad Hoc, Sensor and Ubiquitous Networks. [Online]. Available: http://www.sciencedirect.com/science/article/pii/S0166531609001072

[3] J. Broch, D. A. Maltz, D. B. Johnson, Y.-C. Hu, and J. Jetcheva, “A performance comparison of multi-hop wireless ad hoc network routing protocols,” in *Fourth Annual ACM/IEEE International Conference on Mobile Computing and Networking(Mobicom98), ACM*, 1998.

[4] F. Bai, N. Sadagopan, and A. Helmy, “Important: a framework to systematically analyze the impact of mobility on performance of routing protocols for ad hoc networks,” in *IEEE Information Communications Conference (INFOCOM 2003)*, 2003.

[5] J. Nilsson and U. Sterner, “Robust MPR-based flooding in mobile ad-hoc networks,” in *MILITARY COMMUNICATIONS CONFERENCE, MILCOM*, 2012.

[6] U. Sterner, “Group mobility model,” Swedish Defence Research Agency, Linköping, Sweden, Tech. Rep. FOI Memo 5431, October 2015.

[7] S. A. Williams and D. Huang, “Group force mobility model and its obstacle avoidance capability,” *Acta Astronautica*, vol. 65, no. 7-8, pp. 949 – 957, 2009. [Online]. Available: http://www.sciencedirect.com/science/article/pii/S0094576509000265

[8] A. Komulainen, U. Sterner, and G. Eriksson, “Stochastic channel model,” Swedish Defence Research Agency, Div. of Information and Aeronautical Systems, Linköping, Sweden, Tech. Rep. FOI-RH--1570--SE, January 2015.

[9] F. Eklöf and B. Johansson, “Position distribution service for mechanised units,” Defence Research Establishment, Div. of Command and Control, Linköping, Sweden, Tech. Rep. FOA-R--00-01734-504--SE, December 2000, in swedish.

[10] P. D. Holm, “A new heuristic UTD diffraction coefficient for nonperfectly conducting wedges,” *IEEE Trans. Antennas Propagat.*, vol. AP-48, no. 8, pp. 1211–1219, Aug. 2000.

[11] J. Macker, “Simplified multicast forwarding (SMF),” IETF, Network Working Group, Internet-Draft, January 2012.

[12] T. Clausen and P. Jacquet, “Optimized link state routing protocol(OLSR),” IETF, Network Working Group, RFC 3626, October 2003.

[13] B. Asp, G. Eriksson, and P. Holm, “Detvag-90® — Final Report,” Defence Research Est., Div. of Command and Control Warfare Technology, Linköping, Sweden, Scientific Report FOA-R–97-00566-504–SE, Sep. 1997.

FOI, Swedish Defence Research Agency, is a mainly assignment-funded agency under the Ministry of Defence. The core activities are research, method and technology development, as well as studies conducted in the interests of Swedish defence and the safety and security of society. The organisation employs approximately 1000 personnel of whom about 800 are scientists. This makes FOI Sweden's largest research institute. FOI gives its customers access to leading-edge expertise in a large number of fields such as security policy studies, defence and security related analyses, the assessment of various types of threat, systems for control and management of crises, protection against and management of hazardous substances, IT security and the potential offered by new sensors.

FOI
Swedish Defence Research Agency
SE-164 90 Stockholm

Phone: +46 8 555 030 00
Fax: +46 8 555 031 00

www.foi.se